

Supporting Information

Visualizing localized nematic states in twisted double bilayer graphene

*Zhen-Yu Wang^{a,†}, Jia-Jun Ma^{a,†}, Qianqian Chen^{b,†}, Kefan Wu^a, Shuigang Xu^{c,d}, Qing Dai^e,
Zheng Zhu^{b,f}, Jindong Ren,^{*e} Hong-Jun Gao^{a,f}, Xiao Lin^{*a,f}*

a, Institute of Physics and University of Chinese Academy of Sciences, Chinese Academy of Sciences, Beijing 100190, China

b, Kavli Institute for Theoretical Sciences, University of Chinese Academy of Sciences, Beijing 100190, China

c, Key Laboratory for Quantum Materials of Zhejiang Province, School of Science, Westlake University, Hangzhou 310024, China

d, Institute of Natural Sciences, Westlake Institute for Advanced Study, Hangzhou 310024, China

e, CAS Key Laboratory of Nanophotonic Materials and Devices, CAS Key Laboratory of Standardization and Measurement for Nano-technology, National Center for Nanoscience and Technology, Beijing 100190, China

f, CAS Center for Excellence in Topological Quantum Computation, University of Chinese Academy of Sciences, Beijing, 100190, China

Contents

1. STM results

1.1 Gate-dependent dI/dV spectroscopy at three stacking regions

1.2 LDOS distribution at different layers at $V_g = -30 \text{ V}, 0 \text{ V}, 30 \text{ V}$

1.3 The topography of tDBLG

2. Experimental methods

2.1 Sample preparation

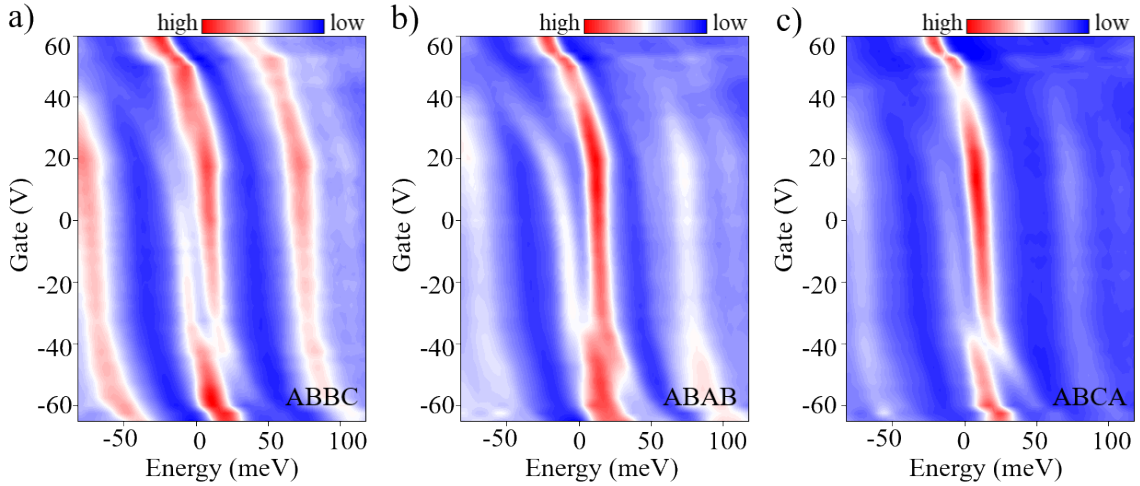
2.2 STM/STS measurements

3. Band structure calculation

1. STM results

1.1 Gate-dependent dI/dV spectra at three stacking regions

We tuned the doping level of the device by varying the back gate voltage and recorded the evolution of flat bands. Figure S1 shows the gate-dependent spectra at three representative regions. We can observe the trends of Δ_V , Δ_C and Δ_{VC} obviously. In the case of Δ_V and Δ_C , the values decrease when increasing back gate voltage, $|V_g|$. While for Δ_{VC} , it shows the asymmetric behavior dependent on the polarity of V_g .



Fi

gure S1. Gate-dependent dI/dV spectra at three stacking regions. (a-c) The dI/dV spectra for ABBC, ABAB and ABCA regions over gate voltage range $-65 \text{ V} < V_g < 60 \text{ V}$. The vertical black dashed line in each figure denotes the Fermi level.

1.2 LDOS distribution at different layers at $V_g = -30 \text{ V}, 0 \text{ V}, 30 \text{ V}$

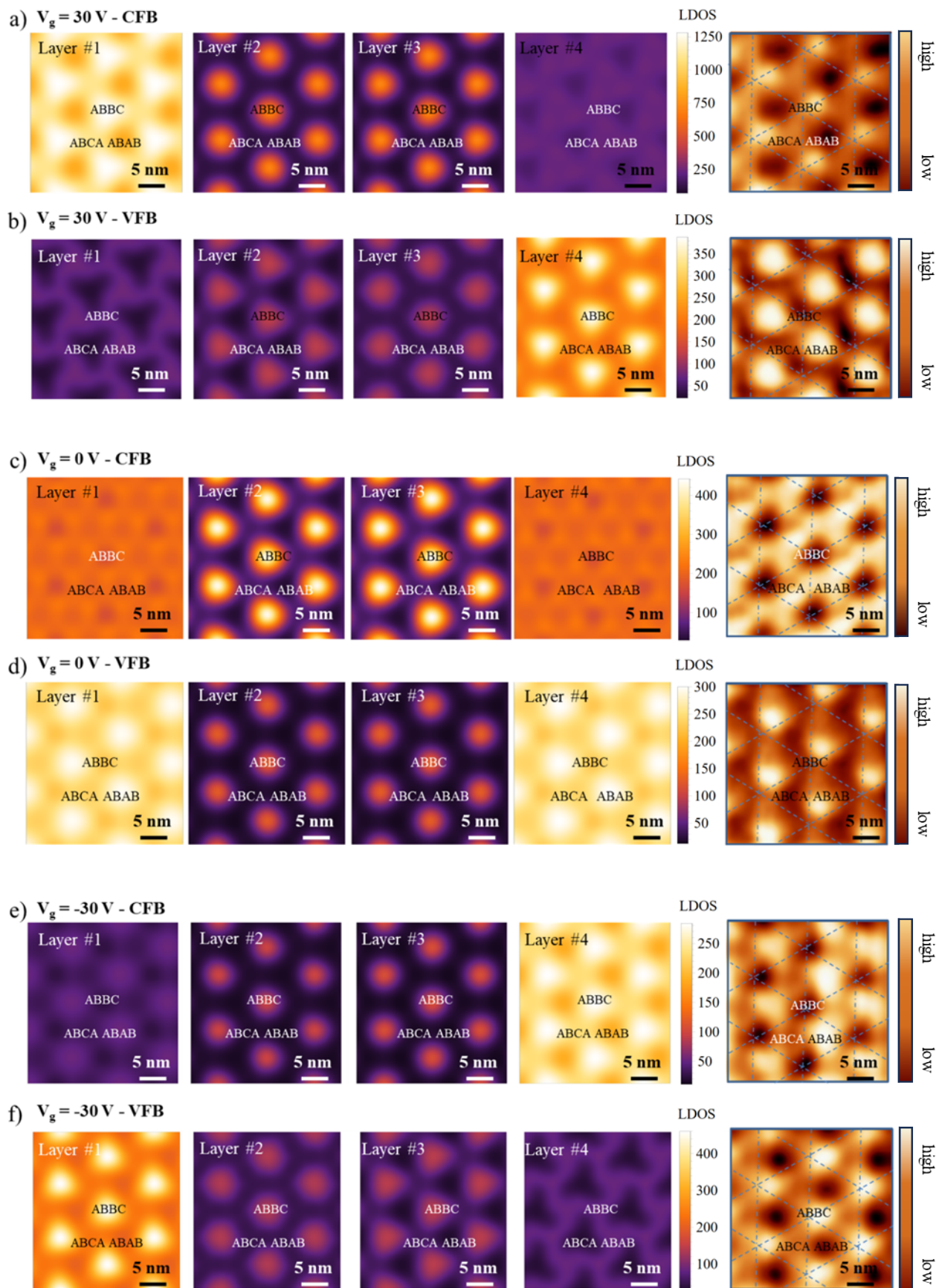


Figure S2. LDOS distribution at different layers after applying different V_g . (a, c, e) The first four images on the left are calculations at the energy of CFB at $V_g = -30$ V, 0 V, 30 V. (b, d, f) The first four images on the left are the simulated topographies located at the energy of VFB at $V_g = -30$ V, 0 V, 30 V. The 5th column image is the experimental STM topography.

1.3 The topography of tDBLG

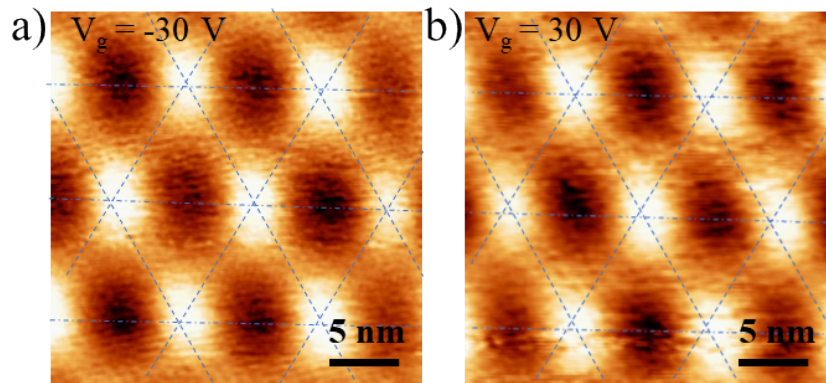


Figure S3. The STM images measured at $V_g = \pm 30$ V. (a, b) The corresponding STM images at $V_g = -30$ V and $V_g = 30$ V. Setpoint for all panels: -0.2 V, 100 pA.

2. Experimental methods

2.1 Sample preparation

The sample in this work was fabricated using a “cut & stack” method developed recently with the assistance of polypropylene carbonate (PPC)/polydimethylsiloxane (PDMS) stamp. A thick h-BN and AB stacking bilayer graphene were exfoliated on SiO_2/Si substrate. The bilayer graphene was cut into two pieces in advance. The h-BN flake was first picked up by PPC. Then, h-BN was used to pick up the first part of the graphene. After the transfer stage was rotated by approximately 1° , the second part of the graphene was picked up. In the above process, the temperature was kept at 40°C . To flip the stack, the PPC film with h-BN/Gr/Gr was transferred to a clean PDMS, with the stack side touching with PDMS. The PPC film can be dissolved by

acetone. Finally, the stack was transferred onto pre-patterned gold electrodes. Another graphite flake was used to connect the graphene and gold electrodes.

2.2 STM/STS measurements

All STM/STS measurements were carried out in a commercial Omicron ultrahigh-vacuum STM held at $T = 5$ K using tungsten (W) tips. The tips were prepared and calibrated on a Au(111) surface to detect the Au(111) Shockley surface state via STS before each set of measurements. dI/dV spectra were recorded using standard lock-in techniques with a bias modulation $V_{\text{RMS}} = 3$ mV at 613.3 Hz. The dI/dV maps were indeed recorded at the energy of the indicated voltage, with a setpoint of -0.2 V and 100 pA for moving the tip to the next point. To obtain these maps, the tip is moved over the surface in a predefined grid, and at each point, the dI/dV vs V spectrum is recorded. This results in a 2D map of the LDOS, which corresponds to the electronic structure of the sample at a specific energy level. A setpoint of -0.2 V and 100 pA was used for moving the tip to the next point.

3. Band structure calculation

We consider a twisted double-bilayer graphene, where one AB-stacked bilayer graphene is stacked on top of another AB-stacked bilayer graphene with a small twist angle θ . We calculate the band structure of the twisted double-bilayer graphene based on the standard moiré bands theory [S1]. The moiré potential reconstructs the original band into a small moiré Brillouin zone (MBZ), which is a hexagon with reciprocal lattice spanned by the moiré basis vectors $b_1^m = \sqrt{3}|\Delta K|(1/2, -\sqrt{3}/2), b_2^m = \sqrt{3}|\Delta K|(1/2, \sqrt{3}/2)$. Here, $|\Delta K| = 2|K|\sin(\theta/2)$ denotes the separation between the Dirac points of the two bilayer graphenes, $K = (4\pi/(3a), 0)$ and

$K' = (-4\pi/(3a), 0)$ are the Dirac points before rotation, and a is the lattice parameter.

The full Hamiltonian for the valley K is:

$$H = H_{BG}^T + H_{BG}^B + H_M.$$

Here, H_{BG}^i is the Hamiltonian of bilayer-graphene (BLG) layer

$$H_{BG}^i = \sum_k \Psi_i^\dagger(k) \begin{pmatrix} U_1 + \Delta & -tf(k, \theta) & \gamma_4 f^*(k, \theta) & \gamma_1 \\ -tf^*(k, \theta) & U_1 & \gamma_3 f(k, \theta) & \gamma_4 f^*(k, \theta) \\ \gamma_4 f(k, \theta) & \gamma_3 f^*(k, \theta) & U_2 & -tf(k, \theta) \\ \gamma_1 & \gamma_4 f(k, \theta) & -tf^*(k, \theta) & U_2 + \Delta \end{pmatrix} \Psi_i(k), \quad i = T, B$$

where $\Psi_i^\dagger(k) = (a_{i1}^\dagger(k), b_{i1}^\dagger(k), a_{i2}^\dagger(k), b_{i2}^\dagger(k))$. The $\Delta = 15$ meV is the onsite energy for the dimer sublattices, U_i is the potential energy difference between two adjacent layers. When expanding

around K , i.e., $k = K + q$, we have $f(k, \theta) = -\frac{\sqrt{3}}{2}a(q_x - iq_y)e^{i\theta}$, where $q = (q_x, q_y)$ has a very small norm.

The interlayer moiré tunnelling term is

$$H_M = \sum_k \sum_{j=0,1,2} (a_{T2}^\dagger(k), b_{T2}^\dagger(k)) T_j \begin{pmatrix} a_{B1}(k + Q_j) \\ b_{B1}(k + Q_j) \end{pmatrix} + \text{h.c.}$$

$$T_j^K = \omega_0 I + \omega_1 \cos\left(\frac{2\pi j}{3}\right) \sigma_x + \omega_1 \sin\left(\frac{2\pi j}{3}\right) \sigma_y, \quad j = 0, 1, 2,$$

where $Q_0 = (0, 0), Q_1 = -b_2^m, Q_2 = b_1^m$. In our calculation, we adopt the parameters extracted from [S2]

$$(t, \gamma_1, \gamma_3, \gamma_4, \omega_0, \omega_1) = (2610, 361, 283, 138, 75, 100) \text{ meV}.$$

The calculated band structure is shown in Figure S4. The two central peaks in Figure 1(e) originate from the flat bands, highlighted in yellow and blue in Figure S4. The other two peaks arise from the band crossings or hybridizations in the remote bands, as depicted in Figure S4.

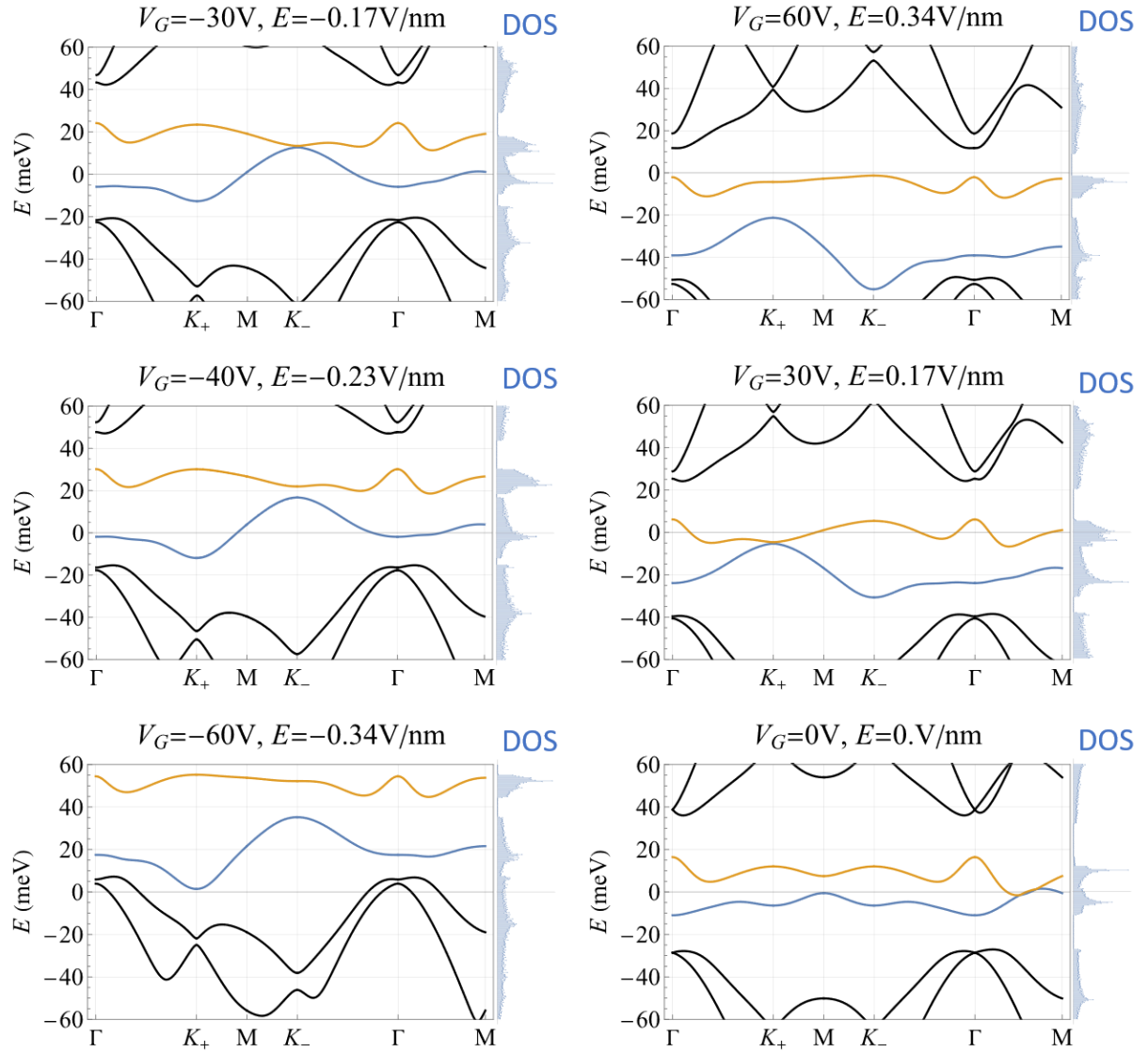


Figure S4. Calculated band structure along the high symmetry directions of the tDBLG moiré Brillouin zone. The yellow bands denote the lowest moiré conduction bands.

References:

[S1] R. Bistritzer and A. H. MacDonald, *Moiré Bands in Twisted Double-Layer Graphene*, Proc. Natl. Acad. Sci. U. S. A. **2011**, *108* (30), 12233-7.

[S2] J. Jung and A. H. MacDonald, *Accurate Tight-Binding Models for the π Bands of Bilayer Graphene*, Phys. Rev. B **2014**, *89* (3), 035405.